Chemical Science

ROYAL SOCIETY OF CHEMISTRY

EDGE ARTICLE

View Article Online
View Journal | View Issue

Cite this: *Chem. Sci.*, 2026, **17**, 6766

All publication charges for this article have been paid for by the Royal Society of Chemistry

Received 20th December 2025
Accepted 2nd February 2026

DOI: 10.1039/d5sc09994c

rsc.li/chemical-science

Photochemical cyclization of α-amino esters to access 3-azetidinones

Meemie U. Hwang,[a] Achyut Gogoi,[bc] Matthew Scurria,[c] Osvaldo Gutierrez*[c] and Karl A. Scheidt *[a]

A light-driven cyclization of readily available α-amino esters to 3-azetidinones has been developed. This method leverages chromophore activation with the acyl imidazole to generate the triplet diradical species under mild conditions without the need for photosensitizers or transition metals. A selective hydrogen atom transfer event, followed by intramolecular Norrish–Yang radical coupling occurs to yield the N-heterocycle, with facile elimination of the imidazole group to access the 3-azetidinone. Computational calculations reveal the role of the protecting group in favoring the Norrish–Yang cyclization pathway.

Introduction

Saturated N-heterocycles are privileged structures frequently encountered in biologically relevant natural products, agrochemicals, and pharmaceuticals.[1] Over the past decade, there has been a significant increase in the prevalence of N-heterocycles in FDA-approved pharmaceuticals, with 82% of drugs containing an N-heterocycle, compared to 59% a decade prior.[2] Notably, saturated N-heterocycles with a higher degree of sp^3-hybridized carbon atoms have seen increased prominence due to the three-dimensional structure which has been linked to improvements in metabolic stability.[3] Among these, the piperidine and pyrrolidine heterocycles are the second and fifth most prevalent in FDA-approved drugs, respectively (Fig. 1A). While azetidines are less frequently utilized in medicinal chemistry, they hold significant potential for enhancing pharmacokinetic properties (Fig. 1B).[4] However, limitations in efficient synthetic routes remain a significant obstacle for the incorporation of azetidines into complex scaffolds.[5] Among azetidine derivatives, compounds featuring carbonyl functional groups at the 2 or 3 positions are of particular interest. The former, 2-azetidinones (β-lactams), have been extensively studied for their antibiotic properties, notably in penicillins, cephalosporins, and monobactams.[6] In contrast, the 3-azetidinone is a significantly underexplored motif in medicinal chemistry as it is not naturally occurring.[7] The 3-azetidinone motif acts as a versatile synthon to enable access to diversified azetidines through various carbonyl functionalization methods.[8] Traditionally, 3-azetidinones can be accessed through formation of the carbon–nitrogen bond with an N–H insertion reaction either through acid-promotion or transition metal catalysis.[5a] An early strategy reported by Correia[9] showcased a [Cu]- or [Rh]-catalyzed carbenoid insertion of α-diazo ketone compounds. However, this methodology requires pre-functionalization with potentially hazardous diazo compounds. In 2011,[10] the Zhang group documented a strategy to avoid diazo intermediates using gold catalysis to achieve the α-oxo metal carbene intermediate, albeit requiring expensive transition metal complexes (Fig. 1C). Addressing the limitations in carbon–nitrogen bond formation of 3-azetidinones poses a challenge and we envisioned that rather a carbon–carbon bond formation could be a potentially advantageous and complimentary strategy[11] to access these underexplored motifs. This carbon–carbon bond formation might be facilitated through the advanced carbonyl triplet diradicals, which have been of interest by our group[12] and others,[13] to induce a regioselective hydrogen atom transfer (HAT) process.

Herein, we present a method from commercially available, abundant α-amino acid esters to access carbonyl triplet diradical reactivity by installing a specific chromophore activation group excited by light. This triplet diradical can subsequently undergo a Norrish–Yang[14] process to form the N-heterocycle and elimination of the chromophore activation group can afford the desired 3-azetidinone product (Fig. 1D).

Our reaction design further envisioned that an activated α-amino acid derivative could be subjected to irradiation to yield the triplet diradical species following intersystem crossing (ISC).[15] A chromophore activation group can induce a bathochromic shift in the absorption profile.[16] This triplet diradical can then undergo a regioselective 1,5-HAT process to form the 1,4-diradical species.[17] Radical–radical coupling, or a Norrish–Yang reaction can afford the 3-azetidinol species and mild basic

[a]*Department of Chemistry, Northwestern University, Evanston, IL 60208, USA. E-mail: scheidt@northwestern.edu*

[b]*Department of Chemistry, Texas A&M University, College Station, Texas, 77843, USA*

[c]*Department of Chemistry and Biochemistry, University of California, Los Angeles, California, 90095, USA. E-mail: o.gutierrez@ucla.edu*

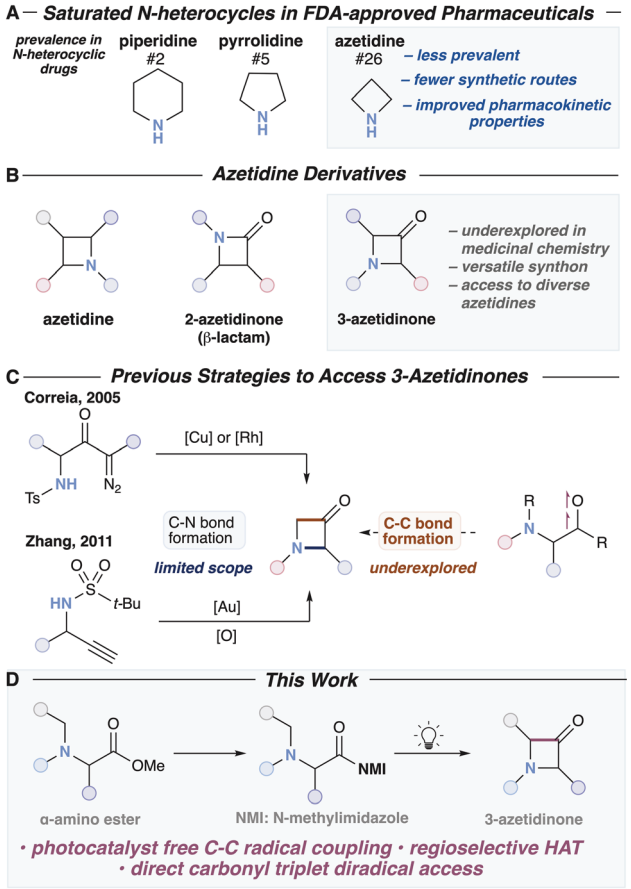

Fig. 1 (A) Saturated N-heterocycles in FDA-approved pharmaceuticals. (B) Azetidine derivatives. (C) Previous strategies to access 3-azetidinones. (D) Synthesis of 3-azetidinones from α-amino acid esters.

conditions can promote nucleophilic elimination to afford the ketone product. To implement this approach, various potential challenges needed to be addressed in substrate design. A variety of chromophore activation groups can be utilized to generate the triplet diradical. The ideal chromophore activation group could induce a bathochromic shift in the absorption profile to facilitate excitation under mild energy light conditions without the need for an external photocatalyst or sensitizer.[16,18] Ideally, the triplet lifetime of the diradical species would be increased following ISC of the excited singlet diradical species. In addition, the group could act as a functional handle to enable further derivatization of the final product. Aromatic ketones have been widely studied as chromophore activation groups to enable various transformations,[13a,19] but do not allow for downstream modulation as a functional handle. In addition, studies from our lab have shown the efficiency of acyl phosphonates[12b,c] and acyl azolium[12a] species as efficient triplet diradical precursors for both intramolecular and intermolecular transformations. Acyl imidazole species have also been utilized as chromophore activators in conjunction with Brønsted acid catalysis[20] for α,β-unsaturated systems to yield the alkene triplet diradical. Once the triplet diradical species is formed, multiple paths of reactivity may occur that can hinder the yield of the desired 3-azetidinone. Achieving control of the competing photochemical processes also present a challenge in substrate development (Fig. 2B). The triplet diradical can undergo either a Norrish type I reaction or an α-cleavage to generate the acyl and α-amino radical species or a Norrish type II fragmentation process to generate the imine and enol species. Site selectivity can also be an obstacle when there are multiple abstractable hydrogen atoms on the substrate.

Results and discussion

We commenced exploration of this triplet cyclization strategy with *N*-benzyl-*N*-tosyl glycine-derived acyl imidazole **1a** in THF. Gratifyingly, irradiation with 370 nm lights for 2 hours yielded the desired 3-azetidinol product **2a** in 71% yield with no detection of Norrish type II fragmentation (Fig. 2C, entry 1). After screening various solvents, it was determined that less polar solvent such as DCM and toluene (Fig. 2C, entries 2 and 3) provided lower yield of the desired product attributed to an increased formation of the Norrish type II fragmentation products. In contrast, polar solvents such as MeCN and DMF provided comparable yields to THF, however use of MeCN induced undesired Norrish type II fragmentation and DMF was suboptimal for purification. Changing the protecting group to a Boc group resulted in no detection of the desired product in THF or DCM, with Norrish type II fragmentation as the primary byproduct. Incorporating α-substitution with the Ts protecting group resulted in only 31% of the cyclized product but a significant yield of the fragmentation product (Fig. 2C, entry 8). Acyl azolium and acyl phosphonate activating groups were also evaluated under these reaction conditions but yielded only the fragmentation product.

With THF as the optimal solvent for the transformation, we explored strategies to remove the imidazole group. Activation of the imidazole with MeOTf in DCM to generate the azolium species **2a′** in 80% isolated yield, followed by mild K_2CO_3 conditions, afforded the 3-azetidinone product **3a** in 27% yield (Fig. 2D). This reaction can also be performed in a single-flask with evaporation of the solvent following MeOTf activation to yield the product in only 18% yield over two steps. These reaction conditions were not ideal for the α-phenyl substituted 3-azetidinol and led to significant decomposition of the product, potentially due to the acidity of the α-position of the final 3-azetidinone product. However, the exploration of the substrate scope revealed that these conditions were broadly tolerated outside of intermediate **2a**.

With the optimal reaction conditions in hand, we evaluated the scope of glycine-derived acyl imidazoles (Fig. 3A). The *N*-Ts-*N*-propyl substrate underwent the desired transformation to yield 3-azetidinol **2b** in good yields. Alkyl substituents, however, did not fully suppress the formation of the Norrish type II byproducts resulting in 57% of **2b** (see SI for details). However, the removal of the imidazole was more effective, yielding the ethyl substituted 3-azetidinone **3b** in 72% yield. Methyl **3c** instead of ethyl 3-azetidinone was also synthesized in good yields. Cyclic substituents were then evaluated to yield

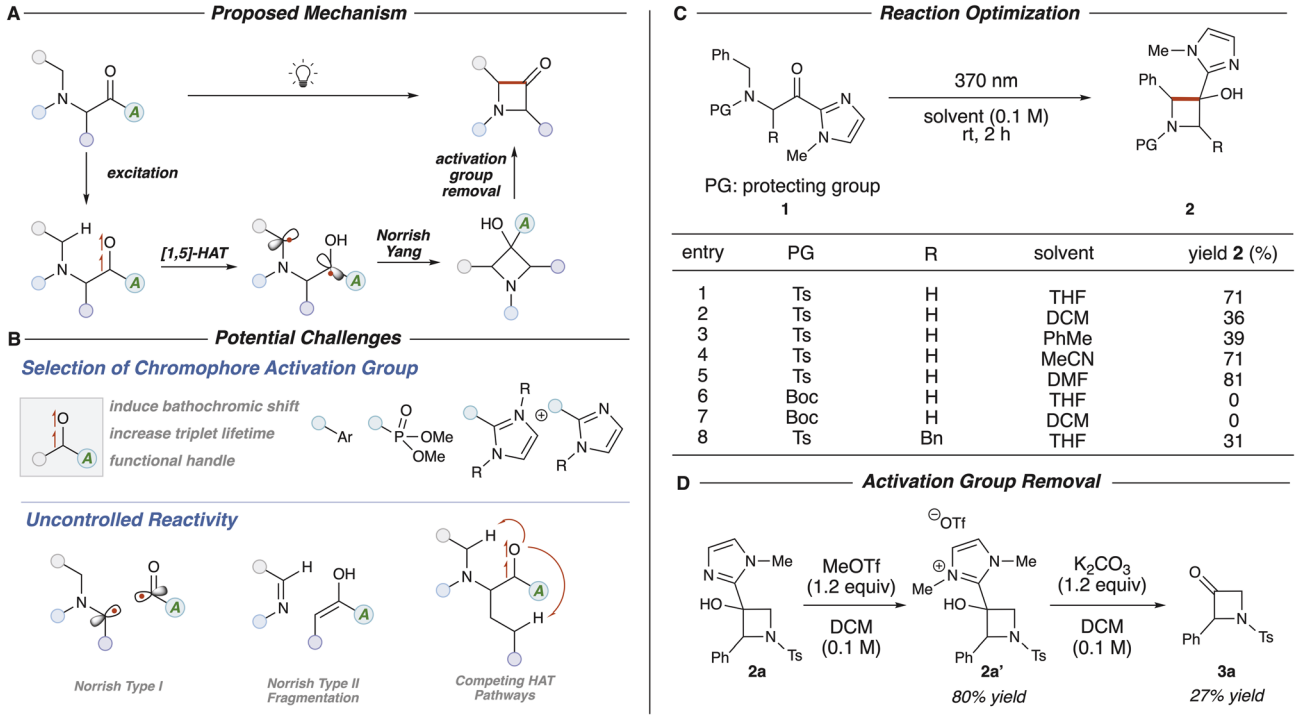

entry	PG	R	solvent	yield **2** (%)
1	Ts	H	THF	71
2	Ts	H	DCM	36
3	Ts	H	PhMe	39
4	Ts	H	MeCN	71
5	Ts	H	DMF	81
6	Boc	H	THF	0
7	Boc	H	DCM	0
8	Ts	Bn	THF	31

Fig. 2 (A) Proposed pathway of the reaction. (B) Potential selectivity challenges. (C) Norrish–Yang photoreaction optimization table. *Reactions conducted at 0.10 mmol scale using acyl imidazole as starting material; yield determined by ^{1}H NMR using 1,3,5-trimethoxybenzene as internal standard. (D) Imidazole group cleavage.

cyclohexyl **3d**, cyclobutyl **3e**, and cyclopropyl 3-azetidinone **3f** in good yields without any observation of the ring opened product during the photoreaction step for **3f**. Benzyl substituted 3-azetidinone **3g** was tolerated in moderate yields.

We then explored various functional groups tolerances. *N*-Ts-*N*-allyl acyl imidazole showed high yields for the photoreaction and resulted in isomerization to the α,β-unsaturated azetidinone **3h** in moderate yields. A 7 : 1 mixture of *E* : *Z* isomers were obtained. Addition of a methylene **3i** and incorporation of a trifluoromethyl group **3j** was also tolerated in good yields. Ester functionalization **3k** was also tolerated, highlighting the selective photoactivity with chromophore activation groups under the standard conditions. A tetrahydropyran motif **3l** also yielded the desired product in good yields as well as a piperidine substrate **3m**. The dioxolane species **3n** was also tolerated and a tertiary radical was also tolerated to yield the *gem*-dimethyl 3-azetidinone **3o**.

Substitution on the α-position was explored to broaden the scope to abundant natural amino acid derivatives (Fig. 3B). Although the incorporation of α-substitution with the tosyl protecting group resulted in minimal Norrish–Yang product formation, changing to the Boc protecting group gratifyingly resulted in the desired azetidinol product. The photoreaction can be tolerated with primary radicals so the methyl group was utilized. *N*-Boc-*N*-methyl alanine acyl imidazole was first tested to yield 73% of the azetidinol product **2p** and 49% yield of 3-azetidinone **3p**. Valine based acyl imidazole **3q** and leucine derived acyl imidazole **3r** were also well tolerated. The 3-azetidinone derived from isoleucine was obtained as a single diastereomer, showing retention of the stereocenter from the amino esters during the photoreaction. In addition, methionine **3t**, phenylalanine **3u**, and TBS protected tyrosine **3u**, were synthesized in good yields. We additionally synthesized the free N–H amino ester and conducted the reaction under standard conditions. Without a protecting group, the photolysis of this substrate resulted in solely Norrish type II fragmentation product with no cyclization detected. 2,4-Disubstituted substrates **2w** and **2x** were also explored and obtained in low yields. Related 2,2-disubstituted substrates however did not result in the desired product.

To expand the synthetic utility of our methodology, we tested a single flask transformation of the desired 3-azetidinone formation (Fig. 4A). Gratifyingly, this transformation was successful, yielding the desired product in 39% yield with one chromatography step as compared to 41% yield utilizing the standard reaction conditions. In addition, the enantioretention of this transformation was evaluated from natural L-phenylalanine (Fig. 4B). The corresponding acyl imidazole **1u** was synthesized with minimal enantioerosion in 97 : 3 e.r. The photochemical step proceeded to afford the 3-azetidinol **2u** in >20 : 1 d.r. The ejection of the imidazole group however, resulted in slight racemization to yield 3-azetidinone **3u** in 75 : 25 e.r. (see SI for more details). The sensitivity of the newly formed stereocenter was unanticipated and provides an interesting opportunity for future development. Synthetic transformations of the 3-azetidinone to biologically relevant functionalized azetidine moieties were performed (Fig. 4C). Nucleophilic addition into the azetidinone **3b** yielded the corresponding

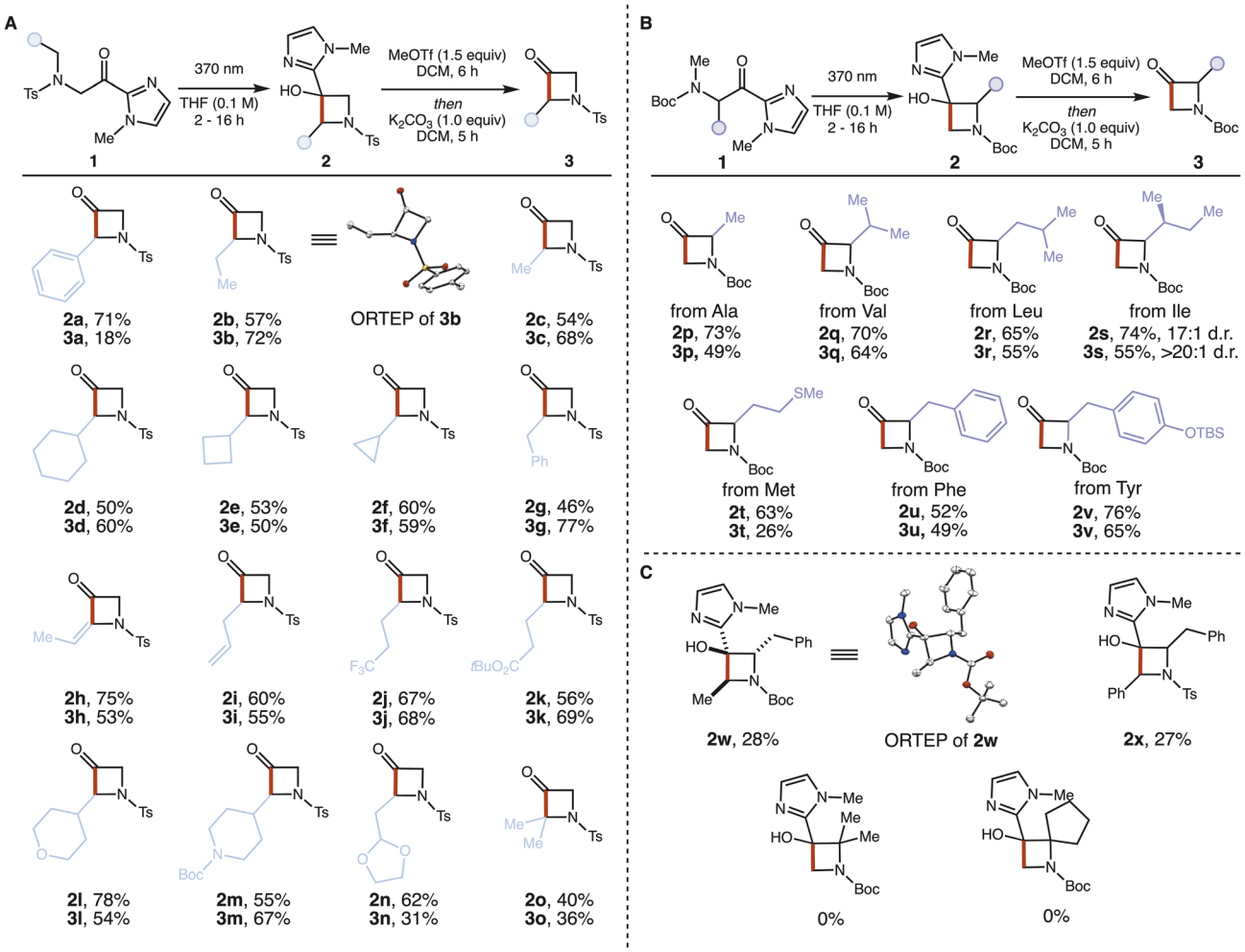

Fig. 3 (A) Ts-protected glycine scope. *d.r. analysis in SI. (B) Boc protected amino ester scope. (C) Unsuccessful substrates.

azetidine **4** in 88% yield. Reduction of the ketone to was also performed to yield the 3-azetidinol **5** in 90% yield in 2.7 : 1 d.r. In addition, the azetidinone could be transformed to the corresponding alkene[21] or 3-dihydropyridinone.[22] Direct substitution of the azolium group utilizing standard K_2CO_3 conditions followed by direct MeMgBr addition yielded **6** in 53% yield and 3 : 1 d.r. *trans* : *cis*.

Several studies were conducted to elucidate the mechanism and determine the sensitivity of this cyclization reaction. Control experiments with the absence of light showed no desired product. A TEMPO trapping experiment was conducted utilizing 3 equivalents of TEMPO to the standard reaction and yielded no desired product. TEMPO adducts of the triplet diradical species was also not observed, consistent with prior intramolecular triplet chemistries. Interestingly, running the reaction under air conditions or adding 10 equivalents of H_2O to the reaction did not affect the yield of the photoreaction. UV-vis spectroscopy studies suggested that the imidazole group acts as a chromophore activator as there is a red-shift in the absorption profile. The aryl ketone **7** also acts as a chromophore activator as compared to the unactivated ester **8**, showing the efficiency of the acyl imidazole group as an aryl ketone surrogate with further synthetic utility.

To elucidate the mechanistic origins and factors governing the preferential formation of the cyclization product over the Norrish type II fragmentation product (Fig. 2B), we employed dispersion-corrected density functional theory (DFT-D3) calculations (see SI for computational details). As shown in Fig. 5A, photoexcitation of intermediate **1A**, followed by intersystem crossing (ISC), generates the triplet species ^{3}**INT1_A**, that has a higher spin density on the carbonyl oxygen than on the carbonyl carbon. This uneven spin distribution facilitates a selective 1,5-hydrogen atom transfer (1,5-HAT) mediated by the oxygen atom, followed by spin crossover to afford ^{1}**INT3_A**, a biradical intermediate, similar to what has been reported before.[12a,b]

In turn, biradical intermediate **INT3_A** can proceed *via* two competing pathways: Norrish–Yang cyclization through ^{1}**TS3_A**, or Norrish type II fragmentation *via* ^{1}**TS3′_A**. Our calculations reveal that the activation barrier for fragmentation is 4.3 kcal mol^{-1} higher than that for cyclization, in agreement with experimental observations. Interestingly, when the tosyl group is replaced with a Boc protecting group, the trend

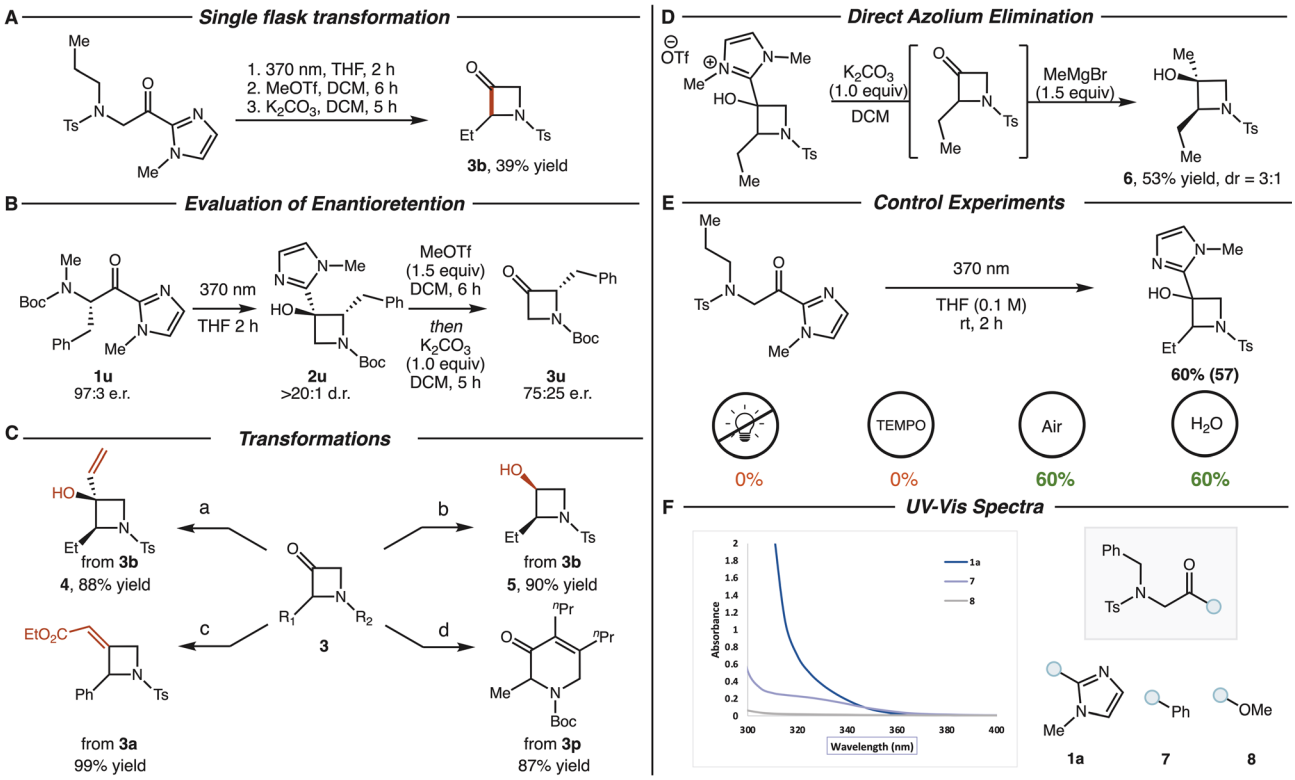

Fig. 4 (A) Single flask transformation. (B) Evaluation of enantioretention. (C) Synthetic transformation conditions: (a) $CH_2CHMgBr$ (1.1 equiv.), THF, −78 °C, 2 h. (b) $NaBH_4$ (1 equiv.), MeOH, r.t., 2 h. (c) See ref. 21. (d) See ref. 22. (D) Direct azolium elimination. (E) Control experiments. (F) UV-vis spectra.

reverses (Fig. 5B), the barrier for fragmentation is 1.6 kcal mol^{-1} lower than for cyclization, consistent with the experimentally observed product distribution. This difference is presumably due to the presence of the carbamate group in the Boc group: the lone pair on the nitrogen (shown in purple in Fig. 5C) is delocalized through resonance with the carbamate moiety of the Boc group, imparting a partial positive charge on the nitrogen atom. This is consistent with our computational atomic charge analysis as well as observed increase in total Wiberg Bond Index (WBI total) on the N atom of the key intermediates (**^{1}INT3_A** and **^{1}INT3_B**) from 3.08 in tosyl-protected substrate to 3.32 in Boc-protected substrate as shown in Fig. 5C (see SI for additional charge analysis).

Natural Bond Orbital (NBO) analysis on the key intermediates **^{1}INT3_A** and **^{1}INT3_B**, which represent the branching point from where the reaction pathways begin to diverge, also support our hypothesis. In the Boc-protected intermediate, we observe significant delocalization of the N lone pair into the empty antibonding orbital of the carbonyl carbon. In strong contrast, the tosyl-protected intermediate shows delocalization of the N lone pair into the half-filled orbital of the adjacent carbon-centered radical, stabilizing the radical and thus favoring cyclization. On the other hand, the Boc-derived delocalization pathway imparts a partial positive charge on the N atom (see SI for more details), increasing its effective electronegativity and destabilizing the radical,[23] thereby promoting fragmentation over cyclization.

Conclusions

We have developed a general cyclization protocol of α-amino esters to 3-azetidinones with a broad substrate scope and moderate to good yields. This method leverages the acyl imidazole as a chromophore activator to allow for direct excitation of the carbonyl for intramolecular HAT and radical coupling. In surprising fashion, the favoring of the cyclization over unproductive fragmentation pathways can be achieved through judicious selection of the tosyl *vs.* Boc protecting groups on the nitrogen atom of the substrate, a key observation that is supported by DFT calculations. Further applications of controlled, direct carbonyl triplet chemistry are underway in our laboratory.

Author contributions

The work was conceptualized by M. U. H. and K. A. S. The experiments were performed by M. U. H. The computational work was done by A. G. and M. S. The manuscript was written through contributions of all authors. K. A. S. and O. G. secured funding and supervised the entire work.

Conflicts of interest

There are no conflicts to declare.

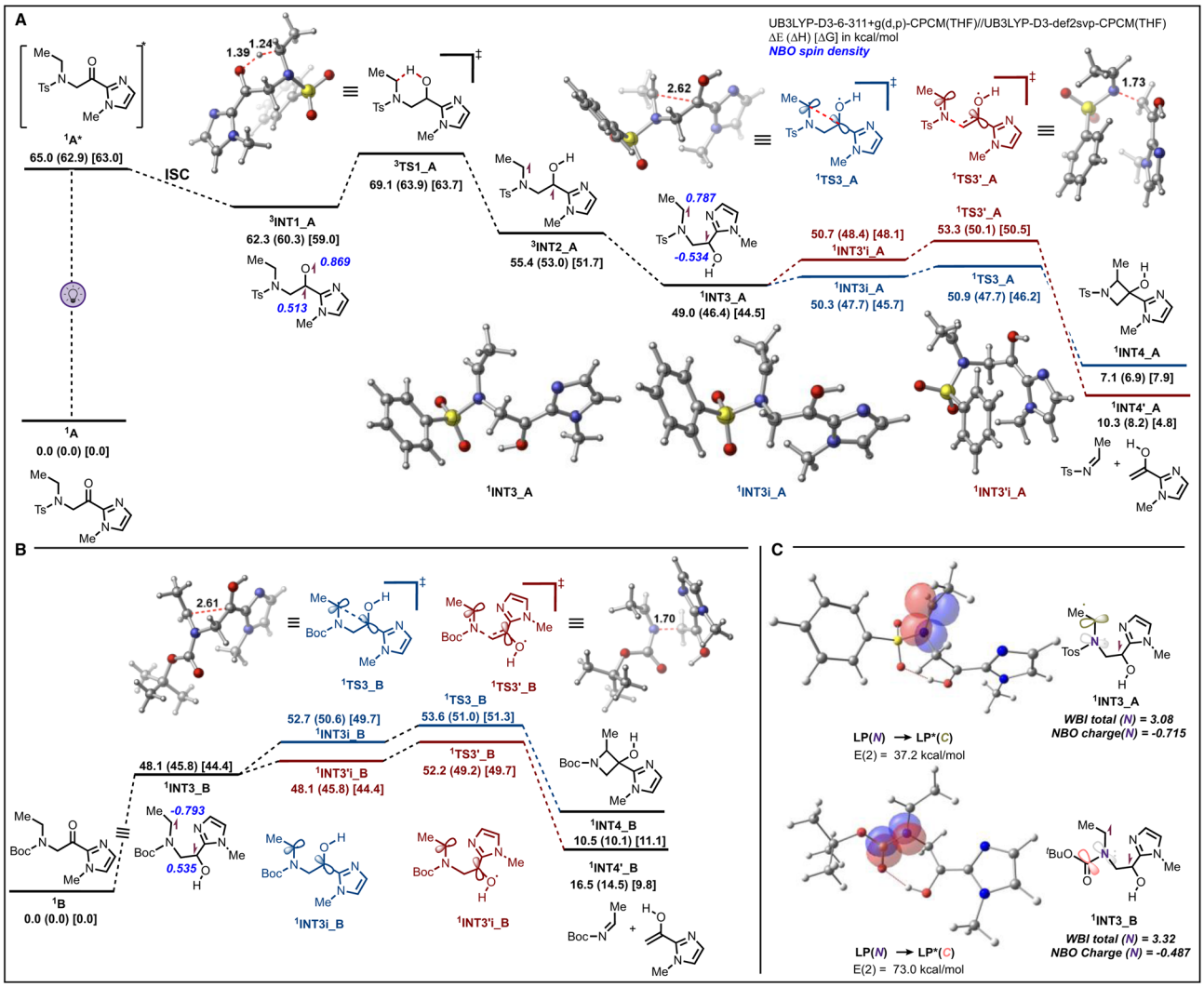

Fig. 5 (A) Minimum energy pathway for formation of Norrish–Yang cyclization product. (B) Norrish–Yang cyclization *vs.* Norrish type II fragmentation pathways for *N*-Boc protecting group. (C) Key NBO interactions leading to the observed divergence for product selectivity between *N*-tosyl *vs. N*-Boc protecting group.

Data availability

CCDC 2463100, 2462978 and 2480795 contain the supplementary crystallographic data for this paper.[24a–c]

The data supporting this article have been included as part of the supplementary information (SI). Supplementary information is available. See DOI: https://doi.org/10.1039/d5sc09994c.

Acknowledgements

The authors thank Northwestern University and the National Institute of General Medical Sciences (R35 GM136440) for support of this work. We thank Charlotte Stern (NU) and Dr Qiupeng Peng (NU) for assistance with X-ray crystallography. We also thank Dr Qiupeng Peng (NU) and Yunchan Nam (NU) for assistance with HRMS. O. G. acknowledges NIH NIGMS (R35 GM137797) for funding and UCLA Hoffman Cluster for computational resources.

Notes and references

1 M. M. Heravi and V. Zadsirjan, *RSC Adv.*, 2020, **10**, 44247–44311.
2 C. M. Marshall, J. G. Federice, C. N. Bell, P. B. Cox and J. T. Njardarson, *J. Med. Chem.*, 2024, **67**, 11622–11655.
3 (*a*) F. Lovering, J. Bikker and C. Humblet, *J. Med. Chem.*, 2009, **52**, 6752–6756; (*b*) F. Lovering, *MedChemComm*, 2013, **4**, 515–519.
4 (*a*) J. T. Lowe, M. D. I. V. Lee, L. B. Akella, E. Davoine, E. J. Donckele, L. Durak, J. R. Duvall, B. Gerard, E. B. Holson, A. Joliton, S. Kesavan, B. C. Lemercier, H. Liu, J.-C. Marié, C. A. Mulrooney, G. Muncipinto, M. Welzel-O'Shea, L. M. Panko, A. Rowley, B.-C. Suh, M. Thomas, F. F. Wagner, J. Wei, M. A. Foley and

L. A. Marcaurelle, *J. Org. Chem.*, 2012, **77**, 7187–7211; (*b*) M. R. Bauer, P. Di Fruscia, S. C. C. Lucas, I. N. Michaelides, J. E. Nelson, R. I. Storer and B. C. Whitehurst, *RSC Med. Chem.*, 2021, **12**, 448–471; (*c*) I. O. Feskov, A. V. Chernykh, Y. O. Kuchkovska, C. G. Daniliuc, I. S. Kondratov and O. O. Grygorenko, *J. Org. Chem.*, 2019, **84**, 1363–1371; (*d*) D. J. St. Jean and C. Fotsch, *J. Med. Chem.*, 2012, **55**, 6002–6020.

5 (*a*) A. Brandi, S. Cicchi and F. M. Cordero, *Chem. Rev.*, 2008, **108**, 3988–4035; (*b*) E. R. Wearing, Y.-C. Yeh, G. G. Terrones, S. G. Parikh, I. Kevlishvili, H. J. Kulik and C. S. Schindler, *Science*, 2024, **384**, 1468–1476; (*c*) R. I. Rodríguez, V. Corti, L. Rizzo, S. Visentini, M. Bortolus, A. Amati, M. Natali, G. Pelosi, P. Costa and L. Dell'Amico, *Nat. Catal.*, 2024, **7**, 1223–1231.

6 L. M. Lima, B. N. M. D. Silva, G. Barbosa and E. J. Barreiro, *Eur. J. Med. Chem.*, 2020, **208**, 112829.

7 Y. Dejaegher, N. M. Kuz'Menok, A. M. Zvonok and N. De Kimpe, *Chem. Rev.*, 2002, **102**, 29–60.

8 (*a*) A. Sharma, A. Choi, D. Yim, H. Kim and H. Kim, *Adv. Synth. Catal.*, 2024, **366**, 2257–2263; (*b*) E. M. Carreira and T. C. Fessard, *Chem. Rev.*, 2014, **114**, 8257–8322.

9 A. C. B. Burtoloso and C. R. D. Correia, *Tetrahedron Lett.*, 2004, **45**, 3355–3358.

10 L. Ye, W. He and L. Zhang, *Angew. Chem., Int. Ed.*, 2011, **50**, 3236–3239.

11 T. Maegawa, K. Otake, K. Hirosawa, A. Goto and H. Fujioka, *Org. Lett.*, 2012, **14**, 4798–4801.

12 (*a*) J. L. Zhu, C. R. Schull, A. T. Tam, A. Renteria-Gomez, A. R. Gogoi, O. Gutierrez and K. A. Scheidt, *J. Am. Chem. Soc.*, 2023, **145**, 1535–1541; (*b*) Q. Peng, A. R. Gogoi, Á. Rentería-Gómez, O. Gutierrez and K. A. Scheidt, *Chem*, 2023, **9**, 1983–1993; (*c*) Q. Peng, M. U. Hwang, Á. Rentería-Gómez, P. Mukherjee, R. M. Young, Y. Qiu, M. R. Wasielewski, O. Gutierrez and K. A. Scheidt, *Science*, 2024, **385**, 1471–1477.

13 (*a*) L. Dell'Amico, J. Mateos, S. Cuadros and A. Vega-Peñaloza, *Synlett*, 2021, **33**, 116–128; (*b*) A. Mavroskoufis, K. Rajes, P. Golz, A. Agrawal, V. Russ, J. P. Gotze and M. N. Hopkinson, *Angew. Chem., Int. Ed.*, 2020, **59**, 3190–3194; (*c*) A. Mavroskoufis, A. Rieck and M. N. Hopkinson, *Tetrahedron*, 2021, **100**, 132497; (*d*) A. Mavroskoufis, M. Lohani, M. Weber, M. N. Hopkinson and J. P. Gotze, *Chem. Sci.*, 2023, **14**, 4027–4037.

14 (*a*) N. C. Yang and D.-D. H. Yang, *J. Am. Chem. Soc.*, 1958, **80**, 2913–2914; (*b*) R. G. W. Norrish and C. H. Bamford, *Nature*, 1937, **140**, 195–196.

15 G. Goti, K. Manal, J. Sivaguru and L. Dell'Amico, *Nat. Chem.*, 2024, **16**, 684–692.

16 C. Brenninger, J. D. Jolliffe and T. Bach, *Angew. Chem., Int. Ed.*, 2018, **57**, 14338–14349.

17 C. Chen, *Org. Biomol. Chem.*, 2016, **14**, 8641–8647.

18 F. Strieth-Kalthoff, M. J. James, M. Teders, L. Pitzer and F. Glorius, *Chem. Soc. Rev.*, 2018, **47**, 7190–7202.

19 (*a*) A. G. Griesbeck and H. Heckroth, *J. Am. Chem. Soc.*, 2002, **124**, 396–403; (*b*) P. J. Wagner, P. A. Kelso, A. E. Kemppainen and R. G. Zepp, *J. Am. Chem. Soc.*, 1972, **94**, 7500–7506; (*c*) H. Zeng, R. Yin, Y. Zhao, J.-A. Ma and J. Wu, *Nat. Chem.*, 2024, 1–9; (*d*) E. H. Gold, *J. Am. Chem. Soc.*, 1971, **93**, 2793–2795; (*e*) P. Wessig and J. Schwarz, *Helv. Chim. Acta*, 1998, **81**, 1803–1814.

20 E. M. Sherbrook, M. J. Genzink, B. Park, I. A. Guzei, M.-H. Baik and T. P. Yoon, *Nat. Commun.*, 2021, **12**, 5735.

21 A. C. B. Burtoloso and C. R. D. Correia, *Tetrahedron*, 2008, **64**, 9928–9936.

22 A. Thakur, J. L. Evangelista, P. Kumar and J. Louie, *J. Org. Chem.*, 2015, **80**, 9951–9958.

23 F. G. Bordwell, X. Zhang and M. S. Alnajjar, *J. Am. Chem. Soc.*, 1992, **114**, 7623–7629.

24 (*a*) CCDC 2463100: Experimental Crystal Structure Determination, 2026, DOI: 10.5517/ccdc.csd.cc2np1v8; (*b*) CCDC 2462978: Experimental Crystal Structure Determination, 2026, DOI: 10.5517/ccdc.csd.cc2nnxx5; (*c*) CCDC 2480795: Experimental Crystal Structure Determination, 2026, DOI: 10.5517/ccdc.csd.cc2p8gn3.